Acoustic Feedback Suppression for Multi-Microphone Hearing Devices Using a Soft-Constrained Null-Steering Beamformer

Henning Schepker, *Member, IEEE*, Sven Nordholm, *Senior Member, IEEE*, and Simon Doclo, *Senior Member, IEEE*

***Abstract*—Acoustic feedback occurs in hearing aids due to the coupling between the hearing aid loudspeaker and microphone(s). In order to reduce the acoustic feedback, adaptive filters are commonly used to estimate the feedback contribution in the microphone(s). While theoretically allowing for perfect feedback cancellation, in practice the adaptive filter typically converges to a biased optimal solution due to the closed-loop acoustical system of the hearing aid. Previously it has therefore been proposed to suppress the acoustic feedback contribution for an earpiece with multiple integrated microphones and loudspeakers using a fixed null-steering beamformer and hence avoiding a biased adaption. While previous null-steering beamforming approaches aimed at perfect preservation of the incoming signal using its relative transfer function (RTF), in this article we propose to use a soft constraint that allows to trade off between incoming signal preservation and feedback suppression. We formulate the computation of the beamformer coefficients both as a least-squares optimization procedure, aiming to minimize the residual feedback power, and as a min-max optimization procedure, aiming to directly maximize the maximum stable gain of the hearing aid. Experimental evaluations were performed using measured acoustic feedback paths from a custom earpiece with two microphones in the vent and a third microphone in the concha. Results show that the proposed fixed null-steering beamformer using the RTF-based soft constraint provides a reduction of the acoustic feedback by 7–8 dB compared to the previously proposed RTF-based hard constraint while limiting the distortions of the incoming signal in the beamformer output.**

***Index Terms*—Acoustic feedback suppression, hearing devices, null-steering beamformer, quadratically constrained quadratic program.**

I. Introduction

ACOUSTIC FEEDBACK occurs due to the coupling between the hearing aid loudspeaker and microphone(s) and may strongly limit the maximum gain of the hearing aid. The signal distortions associated with acoustic feedback are often perceived as whistling or howling. Therefore, in order to increase the maximum applicable gain and maintain a high quality of the signal, robust feedback suppression algorithms are required.

Various approaches for acoustic feedback suppression exist (e.g., [1] and references therein) that include frequency shift, phase modulation as well as notch filtering, adaptive feedback cancellation (AFC) and spatial filtering methods. AFC is considered as one of the most promising methods, where an adaptive filter is used to estimate the acoustic feedback path between the hearing aid loudspeaker and the microphone(s). Subsequently this estimate is used to subtract an estimate of the feedback component from the microphone signal. Theoretically, AFC allows to perfectly remove the feedback component from the microphone signal. However, in practice the adaptive filter estimate is typically biased due to the correlation of the incoming signal and the loudspeaker signal in the closed-loop acoustical system [2], [3]. While several approaches have been proposed that aim at reducing the bias in the filter estimation [3]–[16], recently it has been proposed to exploit multiple microphones of the hearing aid using a fixed beamformer that steers a spatial null into the position of the hearing aid loudspeaker [17], [18]. Since in this approach a fixed processing is applied, the problem of a biased adaptation is avoided.

In order to preserve the incoming signal in the output of the null-steering beamformer, in [18] it has been proposed to use a constraint based on the relative transfer function (RTF) of the incoming signal. While in [18] a hard constraint was used that allowed to perfectly preserve the incoming signal, it may be beneficial to allow for some (inaudible) distortions in the beamformer output to increase the feedback suppression performance. Therefore, in this paper we propose to use a soft constraint based on the RTF of the incoming signal when optimizing the null-steering beamformer. This effectively allows to trade off between feedback suppression performance and incoming signal preservation. In order to select the trade-off parameter, we propose two different selection criteria. The first selection criterion aims at increasing the maximum stable gain (MSG) of the hearing device by a predefined margin compared to the hard-constrained null-steering beamformer. The second selection criterion aims at limiting the amount of distortions of the proposed soft-constrained null-steering beamformer

Manuscript received August 29, 2019; revised January 16, 2020; accepted February 12, 2020. Date of publication February 24, 2020; date of current version March 12, 2020. This work was supported by the Deutsche Forschungsgesellschaft (DFG, German Research Foundation) - Project ID 352015383 - SFB 1330 C1 and Project ID 390895286 - EXC 2177/1. EDICS: AUD-AMHA, AUD-NEFR. The associate editor coordinating the review of this manuscript and approving it for publication was Prof. Tan Lee. *(Corresponding author: Henning Schepker.)*

Henning Schepker and Simon Doclo are with the Signal Processing Group, Department of Medical Physics and Acoustics, University of Oldenburg, 26111 Oldenburg, Germany (e-mail: henning.schepker@uni-oldenburg.de; simon.doclo@uni-oldenburg.de).

Sven Nordholm is with the Faculty of Science and Engineering, Curtin University, Kent Street, Bentley, WA 6102, Australia (e-mail: s.nordholm@curtin.edu.au).

Digital Object Identifier 10.1109/TASLP.2020.2975390

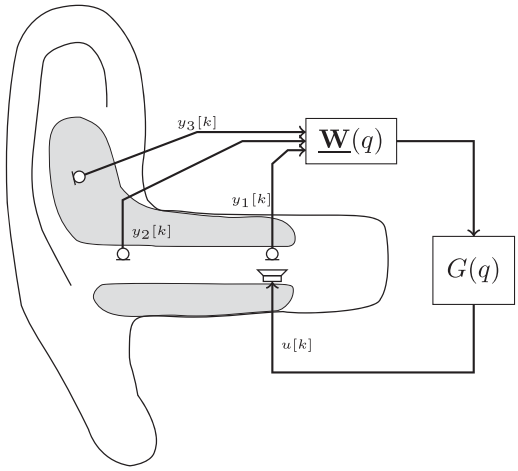

Fig. 1. Considered hearing aid setup with a single-loudspeaker three-microphone earpiece.

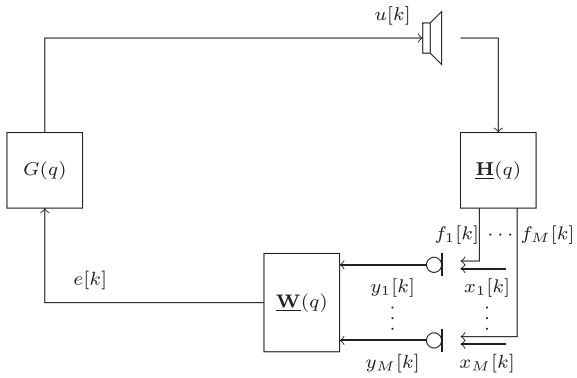

Fig. 2. Considered single-loudspeaker multi-microphone hearing aid system.

compared to the hard-constrained null-steering beamformer in [18]. In order to design the null-steering beamformer, we consider both the minimization of the residual feedback component in the beamformer output as well as the maximization of the MSG. While the minimization of the residual feedback power subject to the RTF-based soft constraint is formulated as a least-squares optimization problem, the maximization of the MSG of the hearing aid subject to the RTF-based soft constraint is formulated as a quadratically constrained quadratic program (QCQP) using the real rotation theorem [19]. Evaluations using measured acoustic feedback paths from a custom three-microphone hearing aid [20], [21] show that using the proposed soft-constrained optimization yields an increase in feedback suppression performance compared to the hard-constrained optimization while maintaining a high quality of the incoming signal in the beamformer output compared to a reference microphone.

This paper is organized as follows. In Section II the acoustic scenario and general notation are introduced. In Section III we briefly review the conditions for perfect feedback suppression and incoming signal preservation based on the closed-loop transfer function of the considered setup. In Section IV we show how the RTF-based soft constraint can be incorporated into the minimization of the residual feedback power as well as the maximization of the MSG. In Section V the proposed RTF-based soft-constrained null-steering beamformer is experimentally compared to the RTF-based hard-constrained null-steering beamformer proposed in [18] in terms of feedback suppression performance and incoming signal preservation. In Section VI we summarize and conclude the paper.

II. Acoustic Scenario and Notation

Consider a single-loudspeaker multi-microphone hearing aid system with M microphones as depicted in Fig. 2. For simplicity we assume that all transfer functions are linear and time-invariant. The mth microphone signal $y_m[k]$, $m = 1, \ldots, M$, at discrete time k is the sum of the incoming signal $x_m[k]$ and the loudspeaker contribution in the mth microphone $f_m[k]$, i.e., using matrix–vector notation

$$\mathbf{y}[k] = \mathbf{x}[k] + \underbrace{\underline{\mathbf{H}}(q)u[k]}_{\mathbf{f}[k]} \tag{1}$$

with

$$\mathbf{y}[k] = [y_1[k] \quad \cdots \quad y_M[k]]^T, \tag{2}$$

$$\mathbf{x}[k] = [x_1[k] \quad \cdots \quad x_M[k]]^T, \tag{3}$$

$$\mathbf{f}[k] = [f_1[k] \quad \cdots \quad f_M[k]]^T, \tag{4}$$

$$\underline{\mathbf{H}}(q) = [H_1(q) \quad \cdots \quad H_M(q)]^T, \tag{5}$$

where $[\cdot]^T$ denotes transpose operation and $u[k]$ denotes the loudspeaker signal. $H_m(q)$ denotes the acoustic feedback path between the mth microphone and the loudspeaker. We assume that it can be modeled as an L_H-dimensional polynomial in q [22], i.e.,

$$H_m(q) = h_{m,0} + \cdots + h_{m,L_H-1}q^{-L_H+1} \tag{6}$$

$$= \mathbf{h}_m^T\mathbf{q}, \tag{7}$$

where $\mathbf{q}$ is the vector containing the delay-elements of q of appropriate length and $\mathbf{h}_m$ denotes the impulse response of the mth acoustic feedback path, i.e.,

$$\mathbf{h}_m = [h_{m,0} \quad \cdots \quad h_{m,L_H-1}]^T. \tag{8}$$

After applying a fixed filter-and-sum beamformer to the microphone signals the beamformer output signal $e[k]$ is obtained, i.e.,

$$e[k] = \underline{\mathbf{W}}^T(q)\mathbf{y}[k], \tag{9}$$

where the $\underline{\mathbf{W}}(q)$ denotes the weighting vector of the beamformer, i.e.,

$$\underline{\mathbf{W}}(q) = [W_1(q) \quad \cdots \quad W_M(q)]^T. \tag{10}$$

The L_W-dimensional beamformer coefficient vector for the mth microphone is defined as

$$\mathbf{w}_m = [w_{m,0} \quad \cdots \quad w_{m,L_W-1}]^T, \tag{11}$$

and the ML_W-dimensional stacked vector of beamformer coefficient vectors is defined as

$$\mathbf{w} = \begin{bmatrix}\mathbf{w}_1^T & \cdots & \mathbf{w}_M^T\end{bmatrix}^T. \tag{12}$$

The beamformer output $e[k]$ is then processed using the hearing aid forward path $G(q)$, yielding the loudspeaker signal $u[k]$, i.e.,

$$u[k] = G(q)e[k]. \tag{13}$$

Furthermore, we assume that the incoming signal $\mathbf{x}[k]$ is composed of a single directional speech source $s[k]$, i.e.,

$$\mathbf{x}[k] = \underline{\mathbf{D}}(q)s[k], \tag{14}$$

where $\underline{\mathbf{D}}(q)$ is the M-dimensional vector containing the acoustic transfer functions (ATFs) between the source and each of the M microphones, i.e.,

$$\underline{\mathbf{D}}(q) = \begin{bmatrix}D_1(q) & \cdots & D_M(q)\end{bmatrix}^T. \tag{15}$$

The L_D-dimensional impulse response vector of the ATF for the mth microphone is defined as

$$\mathbf{d}_m = \begin{bmatrix}d_{m,0} & \cdots & d_{m,L_D-1}\end{bmatrix}^T. \tag{16}$$

The incoming signal $\mathbf{x}[k]$ can also be defined by using the RTFs between a reference microphone m_0 and the remaining microphones, i.e.,

$$\mathbf{x}[k] = \underline{\tilde{\mathbf{D}}}(q)x_{m_0}[k] = \underline{\tilde{\mathbf{D}}}(q)D_{m_0}(q)s[k], \tag{17}$$

where $\underline{\tilde{\mathbf{D}}}(q)$ is the M-dimensional vector containing the RTF between the microphones, i.e.,

$$\underline{\tilde{\mathbf{D}}}(q) = \frac{\underline{\mathbf{D}}(q)}{D_{m_0}(q)}, \tag{18}$$

where $D_{m_0}(q)$ is the ATF between the source and the reference microphone m_0. The $L_{\tilde{D}}$-dimensional impulse response vector of the RTF for the mth microphone is defined as

$$\tilde{\mathbf{d}}_m = \begin{bmatrix}\tilde{d}_{m,0} & \cdots & \tilde{d}_{m,L_{\tilde{D}}-1}\end{bmatrix}^T. \tag{19}$$

In the frequency domain, the beamformer response for the acoustic feedback paths can be computed by applying the N_{FFT}-point discrete Fourier transform (DFT) to the beamformer response in the time-domain, i.e.,

$$\underline{\mathbf{H}}^H(\omega_n)\underline{\mathbf{W}}(\omega_n) = \mathfrak{f}^T(\omega_n)\mathbf{H}\mathbf{w}, \tag{20}$$

where $[\cdot]^H$ denotes the hermitian operator, i.e., complex conjugate transpose, ω_n denotes the nth discrete angular frequency, $\mathfrak{f}(\omega_n)$ is the $(L_H + L_W - 1)$-dimensional vector of the DFT matrix, i.e.,

$$\mathfrak{f}(\omega_n) = \begin{bmatrix}1 & e^{-\frac{j2\pi n}{N_{FFT}}} & e^{-\frac{j2\pi 2n}{N_{FFT}}} & \cdots & e^{-\frac{j2\pi n(L_H+L_W-2)}{N_{FFT}}}\end{bmatrix}^T, \tag{21}$$

and $\mathbf{H}$ is the $(L_H + L_W - 1) \times ML_W$-dimensional matrix of the concatenated $(L_H + L_W - 1) \times L_W$-dimensional convolution matrices $\mathbf{H}_m$, i.e.,

$$\mathbf{H} = \begin{bmatrix}\mathbf{H}_1 & \cdots & \mathbf{H}_M\end{bmatrix}, \tag{22}$$

with

$$\mathbf{H}_m = \begin{bmatrix} h_{m,0} & 0 & \cdots & 0 \\ h_{m,1} & h_{m,0} & \ddots & \vdots \\ \vdots & \ddots & \ddots & \vdots \\ h_{m,L_W-1} & \ddots & \ddots & h_{m,0} \\ \vdots & \ddots & \ddots & \vdots \\ h_{m,L_H-1} & \ddots & \ddots & \vdots \\ \vdots & \ddots & \ddots & \vdots \\ 0 & \cdots & \cdots & h_{m,L_H-1} \end{bmatrix}. \tag{23}$$

III. System Analysis

In the following we analyse the transfer function of the hearing aid system depicted in Fig. 2, similarly as in [18]. By combining (1), (9), and (13) we can rewrite the loudspeaker signal as [18]

$$u[k] = \underbrace{\frac{G(q)\underline{\mathbf{W}}^T(q)}{1 - O(q)}}_{\underline{\mathbf{C}}^T(q)}\mathbf{x}[k], \tag{24}$$

with $O(q)$ the open-loop transfer function defined as

$$O(q) = G(q)\underline{\mathbf{W}}^T(q)\underline{\mathbf{H}}(q), \tag{25}$$

and $\underline{\mathbf{C}}(q)$ the closed-loop transfer function. From this expression it can be observed that perfect feedback suppression and incoming signal preservation for the considered system can be achieved under the following conditions:

- the beamformer $\underline{\mathbf{W}}(q)$ suppresses the feedback contribution in the microphones, i.e.,
$$\underline{\mathbf{W}}^T(q)\underline{\mathbf{H}}(q) = 0. \tag{26}$$
with $W_m(q) \neq 0$ for at least one $m \in [1, \ldots, M]$ to avoid the trivial solution
- the beamformer $\underline{\mathbf{W}}(q)$ preserves the incoming signal in a reference microphone m_0 in its output, i.e.,
$$\underline{\mathbf{W}}^T(q)\mathbf{x}[k] = x_{m_0}[k]. \tag{27}$$

If (26) and (27) hold, then from (24) we obtain

$$u[k] = G(q)x_{m_0}[k] \tag{28}$$
$$= G(q)D_{m_0}(q)s[k]. \tag{29}$$

Furthermore, from (27) and using (17) we can rewrite the condition for the incoming signal preservation as

$$\underline{\mathbf{W}}^T(q)\underline{\mathbf{D}}(q) = D_{m_0}(q)q^{-L_d}, \tag{30}$$

$$\underline{\mathbf{W}}^T(q)\underline{\tilde{\mathbf{D}}}(q) = q^{-L_d}, \tag{31}$$

where the additional delay L_d allows the beamformer $\underline{\mathbf{W}}(q)$ to exploit potential acausalities. Assuming a broadband forward path gain function $G(q) = |G|q^{-d_G}$ with $d_G \geq 1$ a delay, the MSG $\mathcal{M}_i$ of the closed-loop system $\underline{\mathbf{C}}(q)$ in (24) for the ith set of acoustic feedback path measurements can be obtained by

rearranging the magnitude response of the open-loop transfer function $|O(\omega_n)| = 1$ for the broadband gain $|G|$, i.e.,

$$\mathcal{M}_i = \frac{1}{\max\limits_{\omega_n} |(\underline{\mathbf{H}}^{(i)})^H(\omega_n)\underline{\mathbf{W}}(\omega_n)|^2}. \tag{32}$$

Note that, in (32) it is assumed that the phase of the open-loop transfer function is a multiple of 2π, hence providing a worst-case assumption for the MSG. Assuming that for I different sets of measurements, of the acoustic feedback paths the lowest MSG determines the MSG of the hearing aid in challenging conditions we further define the *overall MSG* as

$$\mathcal{M} = \min_i \mathcal{M}_i, \qquad i = 1, \ldots, I. \tag{33}$$

IV. Fixed Null-Steering Beamformer Design

In this section we consider the design of a fixed null-steering beamformer to suppress the feedback contribution of the loudspeaker in the microphones while preserving the incoming signal in the beamformer output. While in [18] a hard constraint was used to preserve the incoming signal, in this paper we relax this requirement and propose to use a soft constraint that allows to trade off between feedback suppression performance and incoming signal preservation. In order to compute the fixed null-steering beamformer, we assume knowledge of multiple (I) sets of acoustic feedback paths $\underline{\mathbf{H}}^{(i)}(q)$, $i = 1, \ldots, I$, e.g., by measurement. This allows to the design the null-steering beamformer to be robust to, e.g., expected changes in the acoustic feedback paths. Furthermore, we assume knowledge of multiple (J) sets of ATFs $\underline{\mathbf{D}}^{(j)}(q)$, $j = 1, \ldots, J$, between the source and the microphones or their corresponding RTFs $\underline{\tilde{\mathbf{D}}}^{(j)}(q)$, which can be obtained, e.g., by in-situ measurement or by selection from a database with measured ATFs/RTFs. These J sets of RTFs could, e.g., correspond to different incoming signal directions. We assume that in a practical scenario all computations required to compute the null-steering beamformer can be performed offline and the obtained fixed coefficients are then transferred to the hearing device. In Section IV-A we present the least-squares optimization problems minimizing the residual feedback power in the beamformer output using either the RTF-based hard constraint or the proposed RTF-based soft constraint. In Section IV-B we present the min-max optimization problems maximizing the MSG of the hearing aid.

A. Minimizing the Residual Feedback Power

To compute the null-steering beamformer cofficients that minimize the residual feedback power while preserving the incoming signal in the beamformer output, we consider the following linearly constrained least-squares optimization problem [18]

$$\boxed{\begin{aligned} &\min_{\mathbf{w}} && \sum_{i=1}^{I} \|(\mathbf{H}^{(i)})\mathbf{w}\|_2^2 && \text{(34a)} \\ &\text{subject to} && \tilde{\mathbf{D}}^{(j)}\mathbf{w} = \check{\mathbf{e}}_{L_d} \quad \forall j = 1, \ldots, J && \text{(34b)} \end{aligned}}$$

where $\|\cdot\|_2$ denotes the l_2-norm, $\mathbf{H}^{(i)}$ is the convolution matrix of the acoustic feedback paths for the ith set of measurements, similarly defined as $\mathbf{H}$ in (22) and $\tilde{\mathbf{D}}^{(j)}$ is the $(L_{\tilde{D}} + L_W - 1) \times ML_W$-dimensional convolution matrix of the jth set of RTFs, i.e.,

$$\tilde{\mathbf{D}}^{(j)} = \begin{bmatrix} \tilde{\mathbf{D}}_1^{(j)} & \cdots & \tilde{\mathbf{D}}_M^{(j)} \end{bmatrix}, \tag{35}$$

with

$$\tilde{\mathbf{D}}_m^{(j)} = \begin{bmatrix} \tilde{d}_{m,0}^{(j)} & 0 & \cdots & 0 \\ \tilde{d}_{m,1}^{(j)} & \tilde{d}_{m,0}^{(j)} & \ddots & \vdots \\ \vdots & \ddots & \ddots & \vdots \\ \tilde{d}_{m,L_W-1}^{(j)} & \ddots & \ddots & \tilde{d}_{m,0}^{(j)} \\ \vdots & \ddots & \ddots & \vdots \\ \tilde{d}_{m,L_{\tilde{D}}-1}^{(j)} & \ddots & \ddots & \vdots \\ \vdots & \ddots & \ddots & \vdots \\ 0 & \cdots & \cdots & h_{m,L_{\tilde{D}}-1}^{(j)} \end{bmatrix}. \tag{36}$$

The $(L_{\tilde{D}} + L_W - 1)$-dimensional vector $\check{\mathbf{e}}_{L_d}$ contains only zeros and a one as the $L_d + 1$th element, i.e.,

$$\check{\mathbf{e}}_{L_d} = [\underbrace{0 \quad \cdots \quad 0}_{L_d} \; 1 \quad 0 \quad \cdots \quad 0]^T. \tag{37}$$

Using a more compact notation, the least-squares optimization problem in (34) can be equivalently written as

$$\boxed{\begin{aligned} &\min_{\mathbf{w}} && \|\tilde{\mathbf{H}}\mathbf{w}\|_2^2 && \text{(38a)} \\ &\text{subject to} && \bar{\mathbf{D}}\mathbf{w} = \bar{\mathbf{e}}_{L_d} && \text{(38b)} \end{aligned}}$$

where $\tilde{\mathbf{H}}$ is the $I(L_W + L_H - 1) \times ML_W$-dimensional matrix of stacked convolution matrices $\mathbf{H}^{(i)}$, i.e.,

$$\tilde{\mathbf{H}} = \begin{bmatrix} (\mathbf{H}^{(1)})^T & \cdots & (\mathbf{H}^{(I)})^T \end{bmatrix}^T, \tag{39}$$

$\bar{\mathbf{D}}$ is the $J(L_{\tilde{D}} + L_W - 1) \times ML_W$-dimensional matrix of stacked convolution matrices $\tilde{\mathbf{D}}^{(j)}$, i.e.,

$$\bar{\mathbf{D}} = \begin{bmatrix} (\tilde{\mathbf{D}}^{(1)})^T & \cdots & (\tilde{\mathbf{D}}^{(J)})^T \end{bmatrix}^T, \tag{40}$$

and $\bar{\mathbf{e}}_{L_d}$ is the $J(L_{\tilde{D}} + L_W - 1)$-dimensional vector of J concatenated vectors $\check{\mathbf{e}}_{L_d}$, i.e.,

$$\bar{\mathbf{e}}_{L_d} = \begin{bmatrix} \check{\mathbf{e}}_{L_d}^T & \cdots & \check{\mathbf{e}}_{L_d}^T \end{bmatrix}^T. \tag{41}$$

The optimal closed-form solution minimizing the least-squares optimization problem in (38) is obtained using the method of Lagrangian multipliers as

$$\mathbf{w} = (\tilde{\mathbf{H}}^T\tilde{\mathbf{H}})^{-1}\bar{\mathbf{D}}^T(\bar{\mathbf{D}}(\tilde{\mathbf{H}}^T\tilde{\mathbf{H}})^{-1}\bar{\mathbf{D}}^T)^{-1}\bar{\mathbf{e}}_{L_d}. \tag{42}$$

Note that in order to compute the solution in (42), the matrix $\tilde{\mathbf{H}}$ needs to be of full column rank, while $\bar{\mathbf{D}}$ needs to be of full row rank. This is equivalent to requiring that the following relationship between the impulse response length L_H, the number of beamformer coefficients L_W, the number of coefficients used to

model the RTF $L_{\tilde{D}}$, the number of measurements I and J and the number of microphones M is satisfied

$$J(L_{\tilde{D}} + L_W - 1) \leq ML_W \leq I(L_W + L_H - 1). \quad (43)$$

While the optimization problem in (38) perfectly preserves the incoming signal in the beamformer output, it limits the amount of feedback suppression that can be performed. Since small distortions of the incoming signal may not be perceivable, we therefore propose to use a soft constraint that effectively allows to trade-off between feedback suppression performance and incoming signal preservation, i.e., we consider the following least-squares optimization problem

$$\boxed{\min_{\mathbf{w}} \quad \|\tilde{\mathbf{H}}\mathbf{w}\|_2^2 + \lambda\|\bar{\mathbf{D}}\mathbf{w} - \bar{\mathbf{e}}_{L_d}\|_2^2} \quad (44)$$

where λ is a real-valued non-negative trade-off parameter. For small values of λ more importance is put on feedback suppression, effectively allowing for more distortions of the incoming signal, while large values of λ yield the opposite effect (cf. also Section V-B). The optimal solution to the optimization problem in (44) is computed as

$$\mathbf{w} = \lambda(\tilde{\mathbf{H}}^T\tilde{\mathbf{H}} + \lambda\bar{\mathbf{D}}^T\bar{\mathbf{D}})^{-1}\bar{\mathbf{D}}^T\bar{\mathbf{e}}_{L_d}. \quad (45)$$

Note that for $\lambda \to \infty$ the solution to the optimization problems in (38) and (44) will be the same [23]. Assuming that either of $\tilde{\mathbf{H}}^T\tilde{\mathbf{H}}$ and $\bar{\mathbf{D}}^T\bar{\mathbf{D}}$ are of full column rank and that $0 < \lambda < \infty$, inversion of $(\tilde{\mathbf{H}}^T\tilde{\mathbf{H}} + \lambda\bar{\mathbf{D}}^T\bar{\mathbf{D}})$ in (45) is possible. Even if both matrices are not of full column rank, using the subadditivity of ranks, we find that in order to compute the inverse in (45), the following inequality needs to hold

$$(M - I - J)L_W \leq I(L_H - 1) + J(L_{\tilde{D}} - 1). \quad (46)$$

B. Maximizing the Maximum Stable Gain

While in Section IV-B the goal was to obtain those null-steering beamformer coefficients that minimize the residual feedback power and preserve the incoming signal, in this section we aim at maximizing the MSG of the hearing aid while preserving the incoming signal. Maximizing the MSG of the hearing aid while perfectly preserving the incoming signal can be formulated as the following linearly constrained min-max optimization problem [18]

$$\boxed{\begin{aligned} \min_{\mathbf{w}} \quad & \max_{\omega_n, i} |(\underline{\mathbf{H}}^{(i)})^H(\omega_n)\underline{\mathbf{W}}(\omega_n)|^2 && (47a)\\ \text{subject to} \quad & \tilde{\mathbf{D}}^{(j)}\mathbf{w} = \check{\mathbf{e}}_{L_d} \quad j = 1, \ldots, J && (47b) \end{aligned}}$$

Using the real rotation theorem [19] the optimization problem in (47) can be approximated with arbitrarily small error as a linear programming problem [18]. The real rotation theorem states that the absolute value of a complex number can be approximated by projecting the complex value onto a rotating complex pointer with discrete rotation angle ϕ_l, $l = 1, \ldots, N_\phi$. By introducing the auxilliary variable t that acts as an upper bound on the optimization, the resulting linear programming formulation is obtained as [18]

$$\min_{t, \mathbf{w}} \quad t \quad (48a)$$

$$\text{subject to} \quad p^{(i)}(\omega_n)\cos\phi_l + q^{(i)}(\omega_n)\sin\phi_l \leq t, \forall\omega_n, i \quad (48b)$$

$$\tilde{\mathbf{D}}^{(j)}\mathbf{w} = \check{\mathbf{e}}_{L_d} \quad j = 1, \ldots, J, \quad (48c)$$

where $p^{(i)}(\omega_n)$ and $q^{(i)}(\omega_n)$ are the real value and imaginary value of the residual beamformer error of the ith measurement, i.e.,

$$p^{(i)}(\omega_n) = \mathfrak{Re}\{(\underline{\mathbf{H}}^{(i)})^H(\omega_n)\underline{\mathbf{W}}(\omega_n)\}, \quad (49)$$

$$q^{(i)}(\omega_n) = \mathfrak{Im}\{(\underline{\mathbf{H}}^{(i)})^H(\omega_n)\underline{\mathbf{W}}(\omega_n)\}. \quad (50)$$

The linear program in (48) can be solved efficiently using existing convex optimization toolboxes, e.g., CVX [24], [25].

Similarly as for the minimization of the residual feedback power in Section IV-A, requiring the incoming signal to be perfectly preserved as in (48) may lead to a limited feedback suppression performance. Therefore, in order to trade off between maximization of the MSG and preservation of the incoming signal, we propose to solve the following optimization problem

$$\boxed{\min_{\mathbf{w}} \quad \max_{\omega_n, i} |(\underline{\mathbf{H}}^{(i)})^H(\omega_n)\underline{\mathbf{W}}(\omega_n)|^2 + \lambda\|\bar{\mathbf{D}}\mathbf{w} - \bar{\mathbf{e}}_{L_d}\|_2^2} \quad (51)$$

where as in (44) λ is a real-valued non-negative trade-off parameter. Similarly as for the least-squares optimization problem in (44), for small values of λ more importance is put on feedback suppression, effectively allowing for more distortions of the incoming signal, while large values of λ yield the opposite effect (cf. also Section V-B).

By introducing the auxiliary variables t and ξ that provide an upper bound in the optimization, the optimization problem in (51) can be equivalently formulated as the following optimization problem

$$\boxed{\begin{aligned} \min_{t, \xi, \mathbf{w}} \quad & t + \xi && (52a)\\ \text{subject to} \quad & |(\underline{\mathbf{H}}^{(i)})^H(\omega_n)\underline{\mathbf{W}}(\omega_n)|^2 \leq t \ \forall\omega_n, i && (52b)\\ & \lambda\|\bar{\mathbf{D}}\mathbf{w} - \bar{\mathbf{e}}_{L_d}\|_2^2 \leq \xi && (52c) \end{aligned}}$$

Similarly as for the RTF-based hard-constrained optimization problem in (48), the optimization problem in (52) can be approximated using the real rotation theorem, leading to the following quadratically constrained quadratic programming (QCQP) problem

$$\min_{t, \xi, \mathbf{w}} \quad t + \xi \quad (53a)$$

$$\text{subject to} \quad p^{(i)}(\omega_n)\cos\phi_l + q^{(i)}(\omega_n)\sin\phi_l \leq t, \quad \forall\omega_n, i \quad (53b)$$

$$\lambda\|\bar{\mathbf{D}}\mathbf{w} - \bar{\mathbf{e}}_{L_d}\|_2^2 \leq \xi. \quad (53c)$$

Similar to the linear program in (48) the QCQP problem in (53) can be solved efficiently using existing convex optimization toolboxes, e.g., CVX [24], [25].

C. Intrusive Trade-Off Parameter Selection

For both soft-constrained optimization procedures, the parameter λ allows to trade off between feedback suppression performance and incoming signal preservation of the null-steering beamformer. The objective is to select λ such that it increases the feedback suppression while maintaining a high quality, i.e., low distortion, of the incoming signal in the beamformer output compared to the incoming signal in the reference microphone m_0. While a large λ may fulfill the objective of incoming signal preservation it may limit the feedback suppression performance. On the contrary, a small λ may lead to a high feedback suppression performance, while strongly distorting the incoming signal. Therefore, a careful selection of the trade-off parameter is required. In the following we present two different selection criteria that relate either to a predefined increase in feedback suppression performance or to a predefined maximum distortion.

When a hearing device is close to instability, increasing the MSG of the hearing device by a predefined margin can be beneficial. Therefore, the first proposed selection criterion aims at increasing in feedback suppression performance in terms of the MSG of the soft-constrained null-steering beamformer compared to the hard-constrained null-steering beamformer. We select the trade-off parameter λ such that the MSG of the soft-constrained null-steering beamformer is approximately ϵ_{MSG} dB larger than the MSG of the hard-constrained null-steering beamformer, i.e.,

$$10\log_{10}\mathcal{M}_{soft} - 10\log_{10}\mathcal{M}_{hard} \approx \epsilon_{MSG}, \tag{54}$$

where $\mathcal{M}_{soft}$ and $\mathcal{M}_{hard}$ denote the MSGs of the soft-constrained optimization procedure and the corresponding hard-constrained optimization procedure, respectively. While this allows to increase the MSG of the hearing device, it may lead to a large reduction of the perceived quality, especially if ϵ_{MSG} is chosen too large. Thus, the second proposed selection criterion aims at limiting the amount of distortions in the beamformer output while increasing the maximum stable gain. We propose to limit the distortion of the incoming signal in the soft-constrained null-steering beamformer output compared to the hard-constrained null-steering beamformer. We select the trade-off parameter such that the normalized distortion for the incoming signal between the hard-constrained null-steering beamformer and the soft-constrained null-steering beamformer is approximately equal to a predefined value, i.e., we choose λ such that

$$10\log_{10}\frac{\|\tilde{\mathbf{D}}\mathbf{w}_{soft} - \tilde{\mathbf{D}}\mathbf{w}_{hard}\|_2^2}{\|\tilde{\mathbf{D}}\mathbf{w}_{hard}\|_2^2} \approx \epsilon_{SD}, \tag{55}$$

where $\mathbf{w}_{soft}$ and $\mathbf{w}_{hard}$ are the beamformer coefficient vectors of the soft-constrained optimization procedure and the corresponding hard-constrained optimization procedure, respectively. In order to select the trade-off parameter λ that yields either the criterion in (54) or (55), we start with a large value of λ and successively decrease λ until the criterion is fulfilled within a margin of 0.5 dB. Speeding up of this process is achieved by first using large steps to decrease λ and then refining the search by using smaller steps.

Note that, when using the proposed selection criterion in (55), the soft-constrained optimization problems in (44) and (53) can be similarly written using a quadratic equality constraint. A typical procedure to minimize convex optimization problems subjected to a quadratic equality constraint is to reformulate them using a soft constraint and finding the optimum trade-off parameter that fullfils the quadratic equality constraint [23]. While for the special case of a least-squares optimization problem with quadratic equality constraint, the optimum trade-off parameter fulfilling the equality constraint can in fact be computed using, e.g., Newtons's method, this is not straight-forward for other convex optimization problems. Hence, while formulating the optimization problem using quadratic equality constraints is possible, here we chose to formulate the optimization problems using a soft constraint to allow for the use of the same selection procedures and criteria for both optimization problems.

V. Experimental Evaluation

In this section the performance of the proposed soft-constrained null-steering beamformer is evaluated when using 2 or 3 microphones and compared with the existing hard-constrained null-steering beamformers [18]. In particular, we consider the ability to suppress the acoustic feedback in different acoustic scenarios as well as the distortion of the incoming signal. When presenting the results we refer to the methods based on minimizing the residual feedback component presented in Section IV-A as LS, while we refer to the methods based on maximizing the maximum stable gain presented in Section IV-B as MM. In Section V-A we describe the acoustic setup and the used performance measures. In Section V-B we show the dependency of the feedback suppression performance and incoming signal preservation on the trade-off parameter λ. In Section V-C the intrusive selection procedures are validated and appropriate values of ϵ_{MSG} and ϵ_{SD} are selected. In Section V-D the optimal performance of the null-steering beamformer is investigated, i.e., the same sets acoustic feedback paths are used for optimization and evaluation. In Section V-E the robustness against changes in the acoustic feedback paths is investigated, i.e., different sets of acoustic feedback paths are used for optimization and evaluation. In Section V-F the perceptual quality and robustness against changes of the incoming signal direction is evaluated.

A. Setup and Performance Measures

Acoustic feedback paths and acoustic transfer functions were measured for the three-microphone-one-loudspeaker earpiece [20], [21] as depicted in Fig. 1 on a dummy head with adjustable ear canals [26]. The impulse responses of the acoustic feedback paths and acoustic transfer functions were sampled at $f_s = 16$ kHz and truncated to length $L_H = 100$ and $L_D = 3000$. Measurements were performed in an acoustically treated chamber ($T_{60} \approx 300$ ms) and the distance between the external source and the dummy head was approximately 1.2 m. Acoustic feedback paths were measured in free-field, i.e., without any obstruction close to the ear, and with a telephone close to the ear. For both conditions ten measurements were performed, where after each measurement the earpiece was removed from the dummy head and reattached, leading to a total of twenty

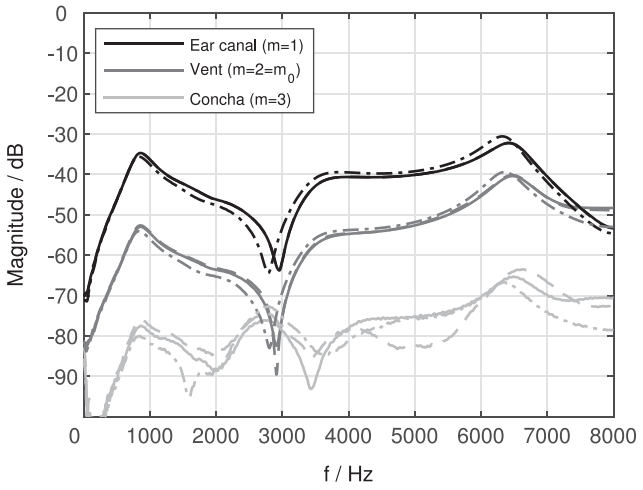

Fig. 3. Magnitude responses of the measured acoustic feedback paths. Continuous lines show exemplary feedback paths measured in free-field, i.e., without any obstruction (used for computing the beamformer coefficients), dashed dotted lines show an exemplary feedback paths after repositioning of the earpiece, and dashed lines show exemplary acoustic feedback paths in the presence of a telephone receiver.

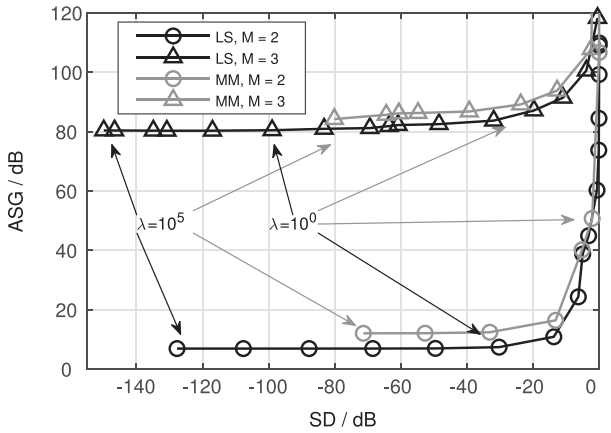

Fig. 4. Dependency of the ASG and the incoming signal distortion on the trade-off parameter λ for the different beamformer optimization problems for an exemplary choice of the beamformer length $L_W = 32$. The value of λ was chosen from $\log_{10}\lambda = \{-10, -9, \ldots, 5\}$.

different feedback path measurements. Four different directions of the incoming signal were considered: frontal, 90 degrees right, back, 90 degrees left. Fig. 3 shows exemplary magnitude responses of the measured acoustic feedback paths for the three different microphones and for different acoustic conditions. The forward path of the hearing aid was set to $G(q) = q^{-96}10^{45/20}$, corresponding to a delay of 6 ms and a broadband amplification of 45 dB. For all experiments the reference microphone $m_0 = 2$, i.e., the microphone located at the outer part of the vent, was chosen since it includes most of the relevant spectral and directional cues and hence provides a natural position for sound pickup. For all min-max optimization problems we used $N_{FFT} = 2048$ discrete frequencies and $N_\phi = 16$ discrete rotation angles to approximate the desired cost function leading to an approximation error of 0.17 dB. In all experiments the RTF of the incoming signal was computed using $L_{\tilde{D}} = 8$, $L_d = 0$ using a regularized least-squares optimization procedure as in [18].

We evaluated the feedback suppression performance of the null-steering beamformer using the added stable gain (ASG) [3], [27], which for the considered hearing aid setup is computed as

$$ASG = 20\log_{10}\frac{1}{\max_{\omega_n}|\underline{\mathbf{H}}^H(\omega_n)\underline{\mathbf{W}}(\omega_n)|} - MSG_{m_0}, \tag{56}$$

where MSG_{m_0} is the MSG of the hearing aid using only the reference microphone m_0, i.e.,

$$MSG_{m_0} = 20\log_{10}\frac{1}{\max_{\omega_n}|H_{m_0}(\omega_n)|}. \tag{57}$$

The amount of the incoming signal distortions SD are evaluated using the normalized squared norm of the difference between the beamformer output and the incoming signal direction, i.e.,

$$SD = \frac{\|\tilde{\mathbf{D}}\mathbf{w} - \tilde{\mathbf{d}}_{m_0}\|_2^2}{\|\tilde{\mathbf{d}}_{m_0}\|_2^2}. \tag{58}$$

Furthermore, we consider the perceptual quality of the signal after applying the null-steering beamformer using the perceptual quality of speech (PESQ) measure [28].

The reference signal for the PESQ measure was the incoming signal $x_{m_0}[k]$ in the reference microphone, while the test signal was the error signal $e[k]$ after applying the beamformer. In order to assess only the effect of the beamformer on speech quality and avoid any influence of the acoustic feedback on the PESQ results, for the perceptual quality evaluation no hearing aid processing was applied, i.e., the hearing aid forward path was set to $G(q) = 0$, and hence $e[k] = \tilde{x}[k]$ in (9). As speech source we used a 80 s long signal obtained by concatenating multiple sentences from different male and female speakers from the TIMIT database [29].

B. Experiment 1: Influence of Trade-Off Parameter

In the first experiment we investigate the influence of the trade-off parameter λ on the feedback suppression performance and the incoming signal preservation. To this end, we compute the null-steering beamformer coefficients using a single measurement of the acoustic feedback paths in free-field and a single frontal incoming signal direction for different values of the trade-off parameter λ and perform the evaluation using the same acoustic feedback paths and ATFs of the incoming signal. Fig. 4 depicts exemplary results for the different optimization problems and numbers of microphones for a beamformer length of $L_W = 32$ in terms of the ASG and the incoming signal distortion SD. For both soft-constrained optimization procedures and numbers of microphones reducing the trade-off parameter λ leads to a substantial increase in the ASG of more than 100 dB. However, this comes at the cost of a reduced quality of the incoming signal as shown by an increased SD.

Comparing the results for both optimization procedures and numbers of microphones it is clear that a fixed choice of λ will yield different improvements for different numbers of microphones and the different optimization problems. This shows

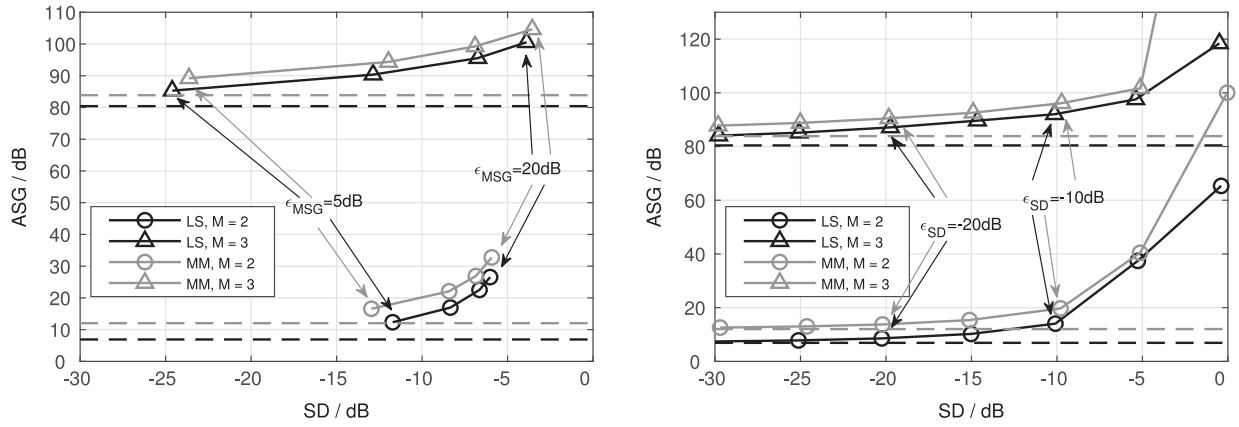

(a) Increased MSG. (b) Allowable distortion.

Fig. 5. ASG and SD as a function of (a) the desired MSG improvement and (b) for the allowable distortion for the different beamformer optimization problems for an exemplary choice of the beamformer length $L_W = 32$. The dashed lines show results for the hard constraint optimization. The performance was evaluated for $\epsilon_{MSG} = \{5, \ldots, 20\}$ dB and $\epsilon_{SD} = \{-30, -25, \ldots, 0\}$ dB.

the need for automatic selection procedures as proposed in Section IV-C.

C. Experiment 2: Intrusive Regularization Parameter Selection

In the second experiment we use the same null-steering beamformer as in the first experiment and validate the intrusive selection procedures outlined in Section IV-C either increasing the MSG by a predefined margin or increasing the incoming signal distortions by a maximally allowed margin. Fig. 5 shows the results for both selection procedures. As can be observed for the selection procedure to increase the MSG in Fig. 5(a), the MSG can be effectively increased by the desired value as indicated by the increased ASG of the soft-constrained optimization procedures compared to the ASG for the hard-constrained optimization procedures. Furthermore, the increase in ASG leads to an expected increase in distortions, with values of up to $SD \approx -5$ dB for a desired MSG increase of 20 dB. Similarly, as can be observed from Fig. 5(b), when the maximum allowed distortion is defined, the desired maximum distortion can be achieved. Note that, as expected, at the same time this also yields an MSG increase as shown by an increased ASG compared to the hard-constrained optimization. Based on these results in the following experiments we will use either a desired MSG increase of $\epsilon_{MSG} = 10$ dB or a maximally allowable distortion of $\epsilon_{SD} = -10$ dB.

D. Experiment 3: Optimal Feedback Suppression Performance

In this experiment we investigate the optimal feedback suppression performance, i.e., when the same acoustic feedback paths are used for optimization and evaluation. Therefore, we will use the ten acoustic feedback paths measured in free-field to compute a single null-steering beamformer and evaluate the performance for the same acoustic feedback paths. Note that in this section we will only consider the ASG and investigate the distortions of the incoming signal in terms of PESQ in Section V-F.

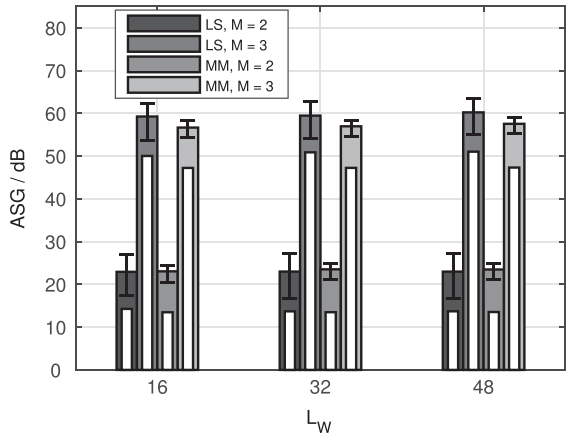

Fig. 6. Feedback suppression performance of the soft-constrained null-steering beamformer in terms of the median ASG as a function of the beamformer length L_W for the different beamformer optimization procedures in Experiment 3 (optimal performance) when an MSG increase of $\epsilon_{MSG} = 10$ dB is desired. Errorbars show minimum and maximum ASG. White bars show the median ASG of the correponding hard-constrained optimization procedures.

Fig. 6 shows the results in terms of the average ASG for the selection procedure using a desired MSG increase of $\epsilon_{MSG} = 10$ dB. While using $M = 2$ microphones yield an average ASG of approximately 23–24 dB, including the third microphone ($M = 3$) yields average ASGs of up to 60 dB. This can be explained by the fact that the third microphone exhibits the smallest feedback component while still containing similar spatial information compared to the microphones in the vent, where the latter is important for a robust preservation of the incoming signal. For all optimization procedures the desired increase of the ASG of about 10 dB compared to the hard-constrained optimization procedures is achieved. Furthermore, as was already observed in [18], there is no large influence of the beamformer length L_W on the feedback suppression performance. In order to investigate the differences between the proposed soft-constrained optimization procedures and the hard-constrained optimization procedures, differences in the ASG are considered

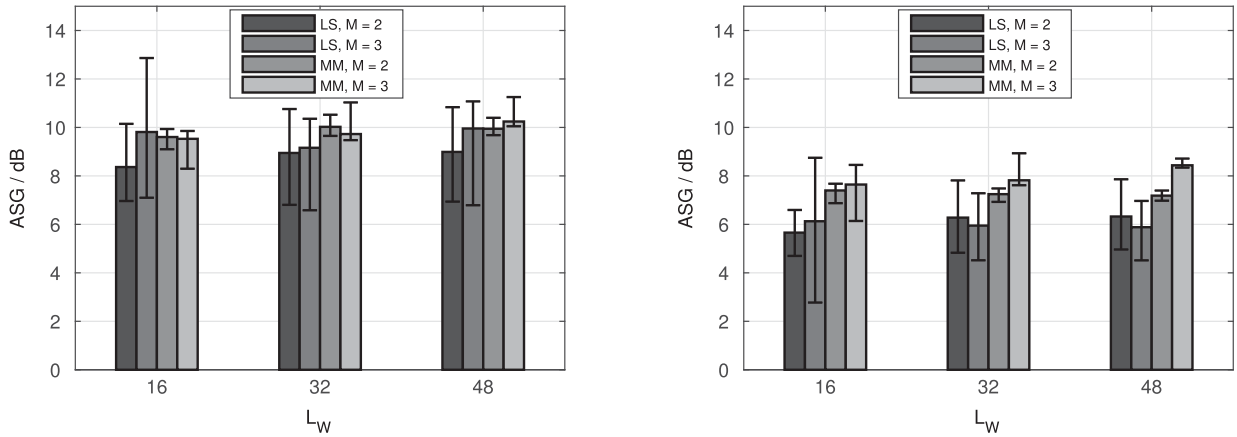

(a) Increased MSG of 10 dB. (b) Allowable distortion of -10 dB.

Fig. 7. Optimal feedback suppression performance (Experiment 3) of the soft-constrained null-steering beamformer in terms of the average improvement in ASG to the hard-constrained null-steering beamformer when (a) an MSG increase of $\epsilon_{MSG} = 10$ dB is desired and (b) the allowable distortions are limited to $\epsilon_{SD} = -10$ dB. Errorbars show the minimum and maximum differences in ASG.

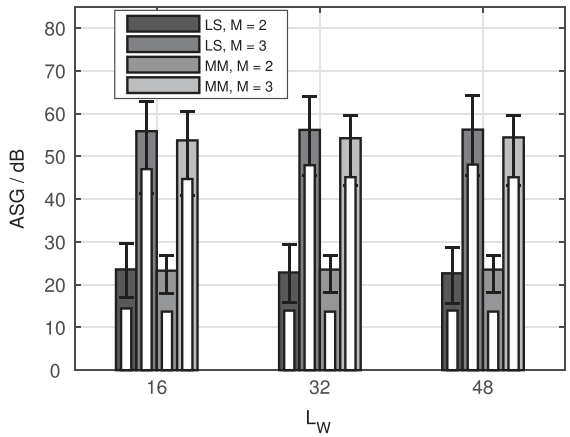

Fig. 8. Feedback suppression performance of the soft-constrained null-steering beamformer in terms of the median ASG as a function of the beamformer length L_W for the different beamformer optimization procedures in Experiment 4 (robust performance) when an MSG increase of $\epsilon_{MSG} = 10$ dB is desired. Errorbars show minimum and maximum ASG. White bars show the median ASG of the correponding hard-constrained optimization procedures.

in the following. Fig. 7(a) shows the average difference in ASG between these optimization procedures. As can be observed on average an increase of 8–10 dB in ASG compared to the hard-constrained optimization procedures can be achieved when using the proposed soft-constrained optimization procedures using the selection procedure based on a desired increased MSG. Note that this increase is not exactly 10 dB since when using multiple sets of acoustic feedback path measurements in the optimization, the criterion in (54) is computed as the overall MSG defined in (33). Hence, when considering differences between the sets for the soft-constrained and the hard-constrained optimization, these differences may not all equal the desired increase in MSG. Fig. 7(b) shows the average improvement in terms of the ASG between the soft-constrained optimization procedures and the hard-constrained optimization procedures for the selection procedure based on a maximum allowable distortion of $\epsilon_{SD} = -10$ dB. As can be observed, allowing for some distortions leads to an average increases of the ASG by about 6–8 dB compared to the hard-constrained optimization procedures. Similarly as before, there is no large influence of the beamformer length L_W on the feedback suppression performance. These results show that in optimal conditions, an average improvement in the ASG can be achieved compared to the hard-constrained optimization procedures when using a soft-constrained optimization procedure. Note that this improvement obviously depends on the desired criterion and hence the selection procedure.

E. Experiment 4: Robust Feedback Suppression Performance

While in the previous experiment the same acoustic feedback paths were used for optimization and evaluation, in practice the acoustic feedback paths will not be the same as used during the optimization. Therefore, in this experiment we investigate the robustness of the null-steering beamformer to unknown acoustic feedback paths. Using the ten sets of acoustic feedback paths measured in free-field, we compute ten different null-steering beamformer using $I = 9$ sets of acoustic feedback paths. We evaluate the performance using the tenth set of acoustic feedback paths, however, instead of using the set of free-field measurements we use the corresponding set of measurements with the telephone receiver in close distance. Thus, this evaluation considers variations of the acoustic feedback paths due to repositioning of the hearing device as well as variations due to the telephone receiver.

Fig. 8 shows the results in terms of the average ASG for the selection procedure based on a desired MSG increase of $\epsilon_{MSG} = 10$ dB. For all optimization procedures an increase in ASG compared to the hard-constrained optimization procedures is achieved. Furthermore, compared to the results of the optimal performance in Experiment 3 shown in Fig. 6, the ASG is smaller for all optimization procedures. In order to investigate the differences between the proposed soft-constrained optimization

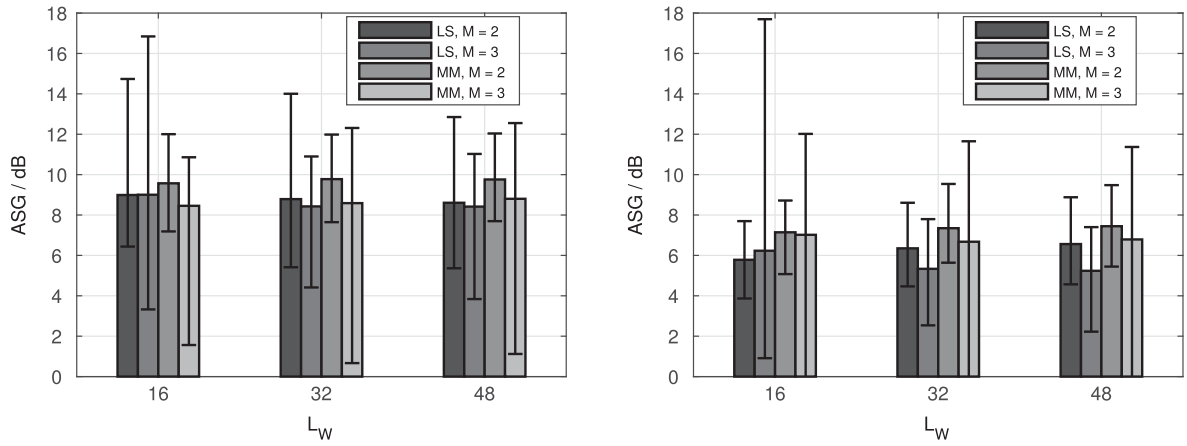

(a) Increased MSG of 10 dB. (b) Allowable distortion of -10 dB.

Fig. 9. Robust feedback suppression performance (Experiment 4) of the soft-constrained null-steering beamformer in terms of the average improvement in ASG to the hard-constrained null-steering beamformer when (a) an MSG increase of $\epsilon_{MSG} = 10$ dB is desired and (b) the allowable distortions are limited to $\epsilon_{SD} = -10$ dB. Errorbars show the minimum and maximum differences in ASG.

procedures and the hard-constrained optimization procedures, Fig. 9(a) shows the average difference in ASG between these optimization procedures. Generally, an increase between 7–9 dB in ASG can be achieved when using the proposed soft-constrained optimization procedures using the selection procedure based on a desired increased MSG.

Fig. 9(b) shows the average improvement in terms of the ASG for the soft-constrained optimization procedure using the selection procedure based on a maximum allowable distortion for $\epsilon_{SD} = -10$ dB compared to the hard-constrained optimization procedure. As can be observed, by allowing for distortions an average improvement in the ASG by about 5–7 dB compared to the hard-constrained optimization procedures can be obtained. Similarly as before, there is no large influence of the beamformer length L_W on the feedback suppression performance. Note that even though for some conditions there is only a small improvement of the soft-constrained min-max optimization procedure compared to the hard-constrained min-max optimization procedure when using $M = 3$ microphones, generally improvements of 6–8 dB are obtained for the soft-constrained optimization procedure compared to the hard-constrained optimization procedure. These results show that using the proposed soft-constrained null-steering beamformer, a robust improvement in the average ASG compared to the hard-constrained null-steering beamformer can be achieved. The magnitude of this improvement obviously depends on the amount of allowable distortions.

F. Experiment 5: Incoming Signal Preservation

While both selection procedures allow to increase the ASG compared to the hard-constrained optimization procedures, they also introduce distortions of the incoming signal. Therefore, in this experiment, the preservation of the incoming signal in the beamformer output is investigated. To this end we use the same ten different null-steering beamformers as in Experiment 4 (cf. Section V-E) and evaluate the performance in terms of PESQ for four different directions of the incoming signal (frontal, right, back, left). Note that only the frontal direction was used in the optimization of the null-steering beamformer.

Fig. 10 shows the PESQ mean opinion scores (MOSs) for both selection procedures. As can be observed from Fig. 10(a), when an MSG increase of 10 dB is desired, the PESQ MOSs are still larger than 4.3 for the frontal direction, which was included in the optimization. For the remaining incoming signal directions, the PESQ MOSs are very similar and generally above 4.3, indicating a high robustness to changes in the incoming signal direction. Furthermore, these results suggest that the lateral incoming signals (right and left) are less affected by the additional distortions that are allowed for by the soft-constrained design. Similar results are observed when the distortion of the incoming signal is limited to -10 dB (cf. Fig. 10(b)). Again for the frontal incoming signal direction PESQ MOSs are similar or larger than 4.3 and for the other directions that were not included in the optimization very similar values are obtained. Comparing the different cost functions (least-squares and min-max) and numbers of microphones, no major differences can be observed. In summary, these results show that the quality of the incoming signal is well preserved, independent of the considered acoustic setup (number of microphones) and optimization criterion, even if the ASG is increased at the cost of additional distortions.

While the results in Fig. 10 show that beamformer does not impact the quality of the incoming signal in the absence of acoustic feedback, this may be different when acoustic feedback is present, i.e., $G_0 > 0$. In order to assess the dependence of the perceived quality on the hearing aid gain G_0, we consider different broadband gains $G(q) = G_0 q^{-d_G}$ with $d_G = 96$ corresponding to a delay of 6 ms, and $G_0 = MSG_{m_0} + \tilde{G}_0$ with $\tilde{G}_0$ the overcritical gain.

Fig. 10 shows the PESQ MOSs for both the hard-constrained least-squares optimization and the soft-constrained least-squares optimization with a desired MSG increase of 10 dB using one exemplary null-steering beamformer computed in Experiment 4 with $L_W = 32$. In order to evaluate the PESQ MOSs we consider an (unknown) incoming signal direction on the right side of the dummy head. As expected, the results show that

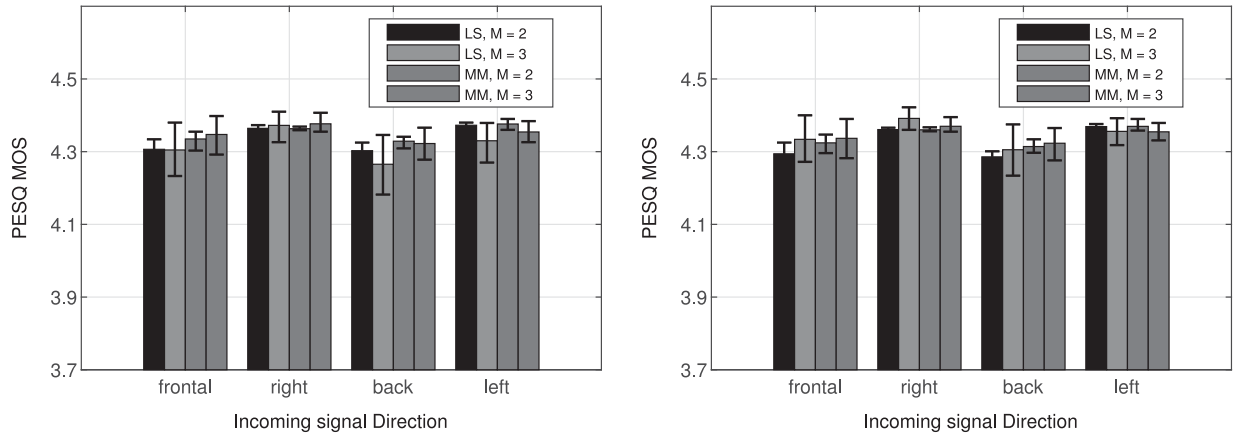

(a) Increased MSG of 10 dB. (b) Allowable distortion of −10 dB.

Fig. 10. Average PESQ MOSs for different incoming signal directions and both optimization procedures for $L_W = 32$ in Experiment 5 when (a) an MSG increase of $\epsilon_{MSG} = 10$ dB is desired and (b) the allowable distortions are limited to $\epsilon_{SD} = -10$ dB. Errorbars show minimum and maximum PESQ MOSs, respectively.

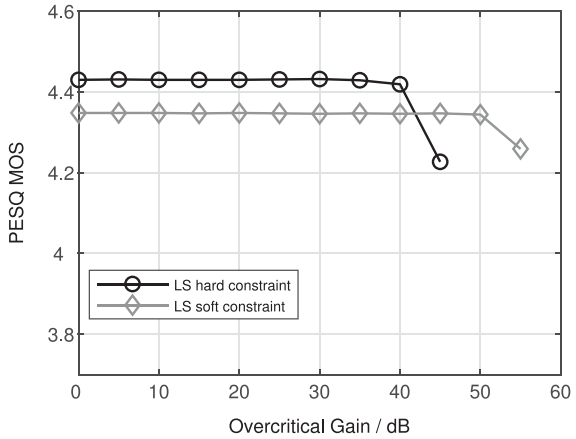

Fig. 11. PESQ MOSs of the incoming signal for different hearing aid gains using $L_W = 32$.

the hard-constrained null-steering beamformer yields a higher quality of the incoming signal compared to the soft-constrained null-steering beamformer for small overcritical gains. Furthermore, while the hard-constrained null-steering beamformer is stable for overcritical gains of up to approximately 45 dB, the soft-constrained null-steering beamformer is stable for overcritical gains of up to 55 dB. This is in line with the ASG results presented Fig. 9(a).

VI. Conclusion

In this paper we considered to use a fixed null-steering beamformer for acoustic feedback suppression in a custom multi-microphone hearing aid that aims to preserve the incoming signal in the beamformer output. While previously a hard constraint was used aiming at perfect preservation of the incoming signal, in this paper we proposed to use a soft constraint that allows to trade off between feedback suppression and incoming signal preservation. We showed how the soft RTF constraint can be incorporated when either minimizing the residual feedback power, leading to a least-squares optimization problem, or maximizing the MSG of the hearing device, leading to a min-max optimization problem. In order to approximate the min-max optimization subject to the proposed soft constraint, we applied the real rotation theorem, leading to a quadratically constrained quadratic program. In order to choose the trade-off parameter, we proposed two different selection procedures that either aim at increasing the feedback suppression performance by a predefined margin, or limiting the distortions of the incoming signal by a predefined margin. Experimental results using measured acoustic impulse responses and acoustic transfer functions from a custom earpiece with three microphones show that using the proposed RTF-based soft constraint yields a larger feedback suppression performance compared to the RTF-based hard constraint, while only introducing minor distortions. This improvement can be as large as 7–8 dB in terms of the median ASG without any significant distortions as indicated by PESQ MOSs generally larger than 4.3.

References

[1] T. van Waterschoot and M. Moonen, "Fifty years of acoustic feedback control: State of the art and future challenges," *IEEE Proc.*, vol. 99, no. 2, pp. 288–327, Feb. 2011.

[2] M. G. Siqueira and A. Alwan, "Steady-state analysis of continuous adaptation in acoustic feedback reduction systems for hearing-aids," *IEEE Trans. Speech Audio Process.*, vol. 8, no. 4, pp. 443–453, Jul. 2000.

[3] A. Spriet, I. Proudler, M. Moonen, and J. Wouters, "Adaptive feedback cancellation in hearing aids with linear prediction of the desired signal," *IEEE Trans. Signal Process.*, vol. 53, no. 10, pp. 3749–3763, Oct. 2005.

[4] A. Spriet, S. Doclo, M. Moonen, and J. Wouters, "Feedback control in hearing aids," in *Proc. Springer Handbook Speech Process.*, J. Benesty, 2008, pp. 979–999.

[5] M. Guo, S. H. Jensen, and J. Jensen, "Novel acoustic feedback cancellation approaches in hearing aid applications using probe noise and probe noise enhancement," *IEEE Trans. Audio. Speech. Lang. Process.*, vol. 20, no. 9, pp. 2549–2563, Nov. 2012.

[6] M. Guo, S. H. Jensen, J. Jensen, and S. L. Grant, "On the use of a phase modulation method for decorrelation in acoustic feedback cancellation," in *Proc. Eur. Signal Process. Conf.*, Bucharest, Romania, Aug. 2012, pp. 2000–2004.

[7] K. Ngo, T. van Waterschoot, M. G. Christensen, M. Moonen, and S. H. Jensen, "Improved prediction error filters for adaptive feedback cancellation in hearing aids," *Signal Process.*, vol. 93, no. 11, pp. 3062–3075, Nov. 2013.

[8] C. R. C. Nakagawa, S. Nordholm, and W. Y. Yan, "Feedback cancellation with probe shaping compensation," *IEEE Signal Process. Lett.*, vol. 21, no. 3, pp. 365–369, Mar. 2014.
[9] F. Strasser and H. Puder, "Sub-band feedback cancellation with variable step sizes for music signals in hearing aids," in *Proc. Int. Conf. Acoust. Speech Signal Process.*, Florence, Italy, May 2014, pp. 8207–8211.
[10] J. M. Gil-Cacho, T. van Waterschoot, M. Moonen, and S. H. Jensen, "Wiener variable step size and gradient spectral variance smoothing for double-talk-robust acoustic echo cancellation and acoustic feedback cancellation," *Signal Process.*, vol. 104, pp. 1–14, Nov. 2014.
[11] C. R. C. Nakagawa, S. Nordholm, and W. Y. Yan, "Analysis of two microphone method for feedback cancellation," *IEEE Signal Process. Lett.*, vol. 22, no. 1, pp. 35–39, Jan. 2015.
[12] H. Schepker, L. T. T. Tran, S. Nordholm, and S. Doclo, "Improving adaptive feedback cancellation in hearing aids using an affine combination of filters," in *Proc. Int. Conf. Acoust. Speech Signal Process.*, Shanghai, China, Mar. 2016, pp. 231–235.
[13] L. T. T. Tran, H. Schepker, S. Doclo, H. H. Dam, and S. E. Nordholm, "Proportionate NLMS for adaptive feedback cancellation in hearing aids," in *Proc. IEEE Int. Conf. Acoust., Speech, Signal Process.*, New Orleans, USA, Mar. 2017, pp. 211–215.
[14] G. Bernardi, T. van Waterschoot, J. Wouters, and M. Moonen, "Adaptive feedback cancellation using a partitioned-block frequency-domain Kalman filter approach with PEM-based signal prewhitening," *IEEE/ACM Trans. Audio Speech Lang. Process.*, vol. 25, no. 9, pp. 1480–1494, Sep. 2017.
[15] S. Nordholm, H. Schepker, L. T. T. Tran, and S. Doclo, "Stability-controlled hybrid adaptive feedback cancellation scheme for hearing aids," *J. Acoust. Soc. Amer.*, vol. 143, no. 1, pp. 150–166, Jan. 2018.
[16] L. T. T. Tran, S. Nordholm, H. Schepker, H. Dam, and S. Doclo, "Two-microphone hearing aids using prediction error method for adaptive feedback control," *IEEE/ACM Trans. Audio, Speech Lang. Process.*, vol. 25, no. 5, pp. 909–923, May 2018.
[17] H. Schepker, L. T. T. Tran, S. E. Nordholm, and S. Doclo, "Combining null-steering and adaptive filtering for acoustic feedback cancellation in a multi-microphone earpiece," in *Proc. Eur. Signal Process. Conf.*, Kos Island, Greece, Aug. 2017, pp. 241–245.
[18] H. Schepker, S. Nordholm, L. T. T. Tran, and S. Doclo, "Null-steering beamformer based feedback cancellation for multi-microphone hearing aids with incoming signal preservation," *IEEE/ACM Trans. Audio Speech, Lang. Process.*, vol. 27, no. 4, pp. 679–691, Apr. 2019.
[19] R. L. Streit, and A. H. Nuttall, "A general Chebyshev complex function approximation procedure and an application to beamforming," *J. Acoust. Soc. Amer.*, vol. 72, no. 1, pp. 181–190, Jul. 1982.
[20] F. Denk, M. Hiipakka, B. Kollmeier, and S. M. A. Ernst, "An individualized acoustically transparent earpiece for hearing devices," *Int. J. Aud.*, vol. 57, no. S3, pp. S62–S70, Jun. 2018.
[21] F. Denk, S. Vogl, H. Schepker, B. Kollmeier, M. Blau, and S. Doclo, "The acoustically transparent hearing device: Towards integration of individualized sound equalization, electro-acoustic modeling and feedback cancellation," in *Proc. Int. Workshop Challenges Hearing Assistive Technol.*, Stockholm, Sweden, Aug. 2017, pp. 89–94.
[22] L. Ljung, *System Identification: Theory for the User*, NJ, USA: Prentice Hall, 1987.
[23] G. H. Golub and C. F. van Loan, *Matrix Computations 3 rd Edition*. Baltimore, MD, USA: The John Hopkins University Press, 1996.
[24] M. Grant and S. Boyd, "Graph implementations of nonsmooth convex programs," in *Recent Advances in Learning and Control*, V. Blondel, S. Boyd, and H. Kimura, Eds. Berlin, Germany: Springer-Verlag, 2008, pp. 95–110, Lecture Notes in Control and Information Sciences.
[25] M. Grant and S. Boyd, "CVX: Matlab software for disciplined convex programming, version 2.1," in Dec. 2016. [Online]. Available: http://cvxr.com/cvx
[26] M. Hiipakka, M. Tikander, and M. Karjalainen, "Modeling the external ear acoustics for insert headphone usage," *J. Audio Eng. Soc.*, vol. 58, no. 4, pp. 269–281, Apr. 2010.
[27] J. M. Kates, "Room reverberation effects in hearing aid feedback cancellation," *J. Acoust. Soc. Amer.*, vol. 109, no. 1, pp. 367–378, Jan. 2001.
[28] "Perceptual evaluation of speech quality (PESQ), an objective method for end-to-end speech quality assessment of narrowband telephone networks and speech codecs," International Telecommunication Union, Geneva, Switzerland, ITU-T Recommendation P.862, 2001.
[29] J. S. Garofolo, "Getting started with the DARPA TIMIT CD-ROM: An acoustic phonetic continuous speech database," *Nat. Inst. Standards Technol.*, Gaithersburg, MD, pp. 1–94, Dec. 1988.

Henning Schepker (Member, IEEE) received the B.Eng. degree from the Jade University of Applied Sciences Oldenburg, Wilhelmshaven, Germany, in 2011 and the M.Sc. degree (with distinction) from the University of Oldenburg, Oldenburg, Germany, in 2012 both in hearing technology and audiology. In 2017, he received the Dr.-Ing. degree from the University of Oldenburg, Germany. He is currently a Postdoctoral Researcher with the Signal Processing Group, Department of Medical Physics and Acoustics, University of Oldenburg, Germany. His research interests are in the area of signal processing for hearing devices and speech and audio applications as well as speech perception.

Sven Nordholm (Senior Member, IEEE) received the MSCEE (Civilingenjör), Licentiate of engineering degrees, and the Ph.D. degree in signal processing from Lund University, Lund, Sweden, in 1983, 1989, and 1992, respectively. Since 1999, he has been a Professor in Signal Processing with the Department of Electrical and Computer Engineering, Curtin University. From 1999 to 2002, he was the Director with ATRI. From 2002 to 2009 he was the Director Signal Processing Laboratory, WATRI, Western Australian Telecommunication Research Institute, a joint institute between The University of Western Australia and Curtin University. He is a Co-founder of two start-up companies; Sensear, providing voice communication in extreme noise conditions and Nuheara a hearables company. His main research efforts have been spent in the fields of Speech Enhancement, Adaptive and Optimum Microphone Arrays, Audio Signal Processing and Acoustic Communication. He has written more than 200 papers in refereed journals and conference proceedings. He contributes frequently in book chapters and encyclopaedia articles and is editor of two special issues on hearing aids and microphone arrays. He is holding seven patents in the area of speech enhancement and microphone arrays. He is an Associate Editor for IEEE/ACM TASPL.

Simon Doclo (Senior Member, IEEE) received the M.Sc. degree in electrical engineering and the Ph.D. degree in applied sciences from the Katholieke Universiteit Leuven, Leuven, Belgium, in 1997 and 2003, respectively. From 2003 to 2007 he was a Postdoctoral Fellow with the Research Foundation Flanders with the Electrical Engineering Department (Katholieke Universiteit Leuven) and the Cognitive Systems Laboratory (McMaster University, Canada). From 2007 to 2009 he was a Principal Scientist with NXP Semiconductors in Leuven, Belgium. Since 2009, he has been a Full Professor with the University of Oldenburg, Germany, and a Scientific Advisor for the Division Hearing, Speech and Audio Technology of the Fraunhofer Institute for Digital Media Technology. His research activities center around signal processing for acoustical and biomedical applications, more specifically microphone array processing, speech enhancement, active noise control, acoustic sensor networks and hearing aid processing. He received several best paper awards (International Workshop on Acoustic Echo and Noise Control 2001, EURASIP Signal Processing 2003, IEEE Signal Processing Society 2008, VDE Information Technology Society 2019). He is member of the IEEE Signal Processing Society Technical Committee on Audio and Acoustic Signal Processing, the EURASIP Technical Area Committee on Acoustic, Speech and Music Signal Processing and the EAA Technical Committee on Audio Signal Processing. He was and is involved in several large-scale national and European research projects (ITN DREAMS, Cluster of Excellence Hearing4all, CRC Hearing Acoustics). He was Technical Program Chair of the IEEE Workshop on Applications of Signal Processing to Audio and Acoustics in 2013 and Chair of the ITG Conference on Speech Communication in 2018. In addition, he served as a Guest Editor for several special issues (IEEE Signal Processing Magazine, Elsevier Signal Processing) and was an Associate Editor for the IEEE/ACM TRANSACTIONS ON AUDIO, SPEECH AND LANGUAGE PROCESSING and *EURASIP Journal on Advances in Signal Processing*.